Journal of Energy and Economic Development,
Niroo Research Institute.
Vol. 1, Issue. 2, Autumn 2022 , Pages 16-30
Journal homepage: https://jeedev.nri.ac.ir

Stochastic Downside Risk-Constrained Scheduling for a Sustainable Power System

Seyedeh Soudabeh Zadsar*[1], Masoud Rashidinejad[2], Amir Abdolahi[3], Sobhan Dorahaki[4], Mohammad Reza Salehizadeh[5]

1. PhD candidate, Department of Electrical Engineering, Shahid Bahonar University of Kerman, Iran,

2. Professor, Department of Electrical Engineering, Shahid Bahonar University of Kerman, Iran,

3. Professor, Department of Electrical Engineering, Shahid Bahonar University of Kerman, Iran,

4. PhD candidate, Department of Electrical Engineering, Shahid Bahonar University of Kerman, Iran,

5. Assistant Professor, Department of Electrical Engineering, Islamic Azad University, Marvdasht, Iran

Original Article

Abstract. With the restrictions on non-renewable energy sources and increasing environmental pollution, attention is being drawn to renewable energy sources. But due to the variable nature of these sources, new challenges have been created in the balance between the production and consumption of power systems. An example of a sustainable energy system (SES) in this paper stores wind power with an electrical energy storage system (EESS) and uses a responsive load economic model (RLEM) to cope with the variable nature of wind generation (WG) and demand. First, since wind energy and demand face uncertainties, the Bayesian probabilistic method is applied to produce the scenario tree. Due to the many generated scenarios, the K-Means clustering algorithm is used to select only 5 scenarios. Furthermore, the downside risk constraints (DRC) method is used to measure the risk imposed by stochastic parameters. The proposed strategy is compared with a risk-neutral strategy to investigate DRC implementation. The results are compared in two cases to demonstrate the advantages of the proposed risk evaluation method. In addition, the Pareto front can be used between risk-in-cost (RIC) and the expected operation cost (EOC) to establish an optimal risk strategy in the presence of uncertainties. The results show that the expected operating cost of the system increases slowly while the expected risk-in-cost of the system decreases significantly.

Keywords: *sustainable energy system, responsive load economic model, Downside risk constraints, Bayesian probabilistic method, K-Means clustering algorithm*

INTRODUCTION

In recent decades, public concern about climate change and the reduction of fossil fuels has led to significant investments in renewable energy production (He et al., 2018). Therefore, the variety of renewable energy sources has created substantial challenges for the power system (Du et al., 2018). Using renewable energy sources (RES), such as solar and wind energy, is fundamental for SES development (Raj et al., 2011).

* *an early version of this paper was presented in International Power System Conference(PSC)*
Corresponding author E-mail addresses: zadsars@yahoo.com
Received Date :2022-09-06;Revised Date:2022-12-05;Accepted Date:2022-12-05
https://doi.org/10.30503/jeedev.2022.360879.1019

A sustainable energy system can be viewed as an extension of distributed generation as it can meet local energy demands with renewable energy or high-efficiency polygeneration production technologies, or both.

Furthermore, it is characterized by energy and cost efficiency, reliability, and environmental friendliness(Rong & Lahdelma, 2016).Additionally,operation improvement can be accomplished through the design of new markets. This can include flexible ramping markets (Beibei Wang & Hobbs, 2013; Navid & Rosenwald, 2012), coordination of demand response (DR) and wind energy (De Jonghe et al., 2014; Hajibandeh et al., 2019), and coordinated operation of the energy storage system using wind farms (Daneshi & Srivastava, 2012). Ref. (Heydarian-Forushani et al., 2015) examined the impact of participating in the energy and reserve market DR with wind energy integration on system operation costs. To deal with the uncertainties of price and WG in the SCUC problem, a bi-level model was studied in (Sahin et al., 2013), considering price-based and incentive-based DR. In (Nazari-Heris et al., 2017), the effect of the DR program was studied on optimal power operation and heat micro-grids, considering the uncertainties of load demand and market price. In (Liu & Tomsovic, 2014), a full DR model was introduced to participate in both the energy and spinning reserve markets simultaneously. Many pieces of research have focused on the effect of energy storage systems on the cost of operation and wind spillage reduction. To solve stochastic unit commitment, the impact of pumped hydro storage units on wind power dispatch was determined in (Khodayar et al., 2013). In (Taljan et al., 2008), a hybrid WG and a nuclear power plant were studied for the economic analysis of hydrogen generation and storage. For this study, the uncertainty and risks of WG were ignored. Lastly, hybrid models of WG, PV systems, batteries, hydrogen generation, and storage units were studied in (Marchenko & Solomin, 2017) to reduce harmful emissions and carbon dioxide. The mentioned work also ignored related uncertainties and risks. In general, having access to a responsive load economic model (RLEM) greatly contributes to our knowledge about the impact of consumer participation in DR programs and their influence on the load profile (Aalami et al., 2010). To handle the uncertainty of day-ahead electricity prices, and to cope with financial losses, a risk management strategy was proposed in (Fotouhi Ghazvini et al., 2015) for an electricity retailer. This study used two-stage stochastic programming to explain the incentive-based DRP and the optimal schedule of retailer generation units and energy storage.

To manage risk, an efficient and straightforward risk measurement method is required, such as the one outlined in (Deng et al., 2020). This method is called the downside risk constraints method. In this paper, due to the variable nature of wind production and demand, the storage system and the responsive load economic model (RLEM) are used. As we know, various scenario-based stochastic programming methods have found application in uncertainty modelling problems. So, the Bayesian probabilistic method is used to model wind and demand uncertainties. The downside risk constraints method is proposed in this paper as a simple risk measurement approach to measure the risk imposed by stochastic parameters. Therefore, in the first step, we suggest using downside risk constraints to manage the risk associated with wind and demand uncertainties. In the second step, comparing WG and EESS hybrid strategies with risk-neutral strategies is proposed. Finally, mixed-integer linear programming (MIP) is used for modelling, which assures finding the optimal global results, and is then solved by the CPLEX solver of GAMS software. Therefore, the novelties and contributions of this paper can be categorized as follows:

- Use of the Bayesian probabilistic method for wind energy and demand uncertainty modelling.

- Use of the K-Means clustering algorithm to reduce the number of total scenarios to 5 with a different probability.
- Proposing downside risk constraints for managing the risk associated with uncertainties.
- Proposing the risk-averse strategy of hybrid WG and EESS versus risk-neutral strategy.

The remaining of this paper is organized as follows:

In section 1, the problem formulation is presented. That includes the model of EESS and WG, considering the responsive load economic model (RLEM). Section 2 presents a general explanation for the downside risk-constrained method. The numerical results of case studies are presented in the numerical studies section. Finally, last section concludes the paper.

1. PROBLEM FORMULATION

According to Fig. 1, the problem of the desired integrated system in the presence of ESS, WG, and the responsive load economic program is formulated in this section.

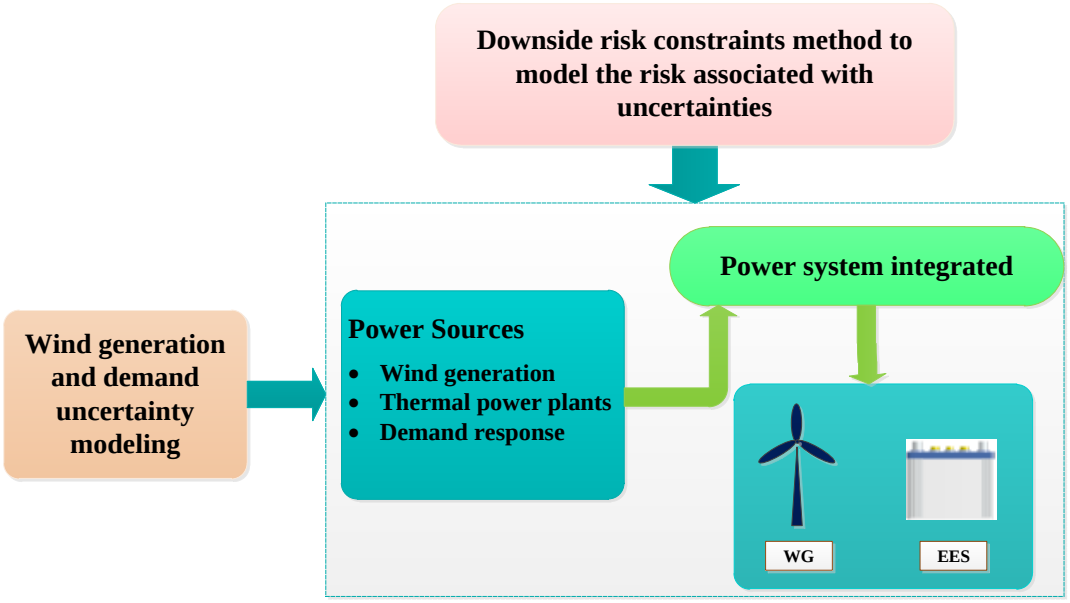

Figure 1. Scheme of the proposed sustainable power system

1.1 Objective Function

The objective function of the proposed model is provided as follows:

$$\text{Min Cost} = \sum_{s=1}^{N_s} \omega_s \sum_{t=1}^{N_t} \left[\sum_{es=1}^{N_{es}} \left(Cost_{es,t,s} \right) + \sum_{i=1}^{N_i} \left(\text{OCT}_{i,t,s} + \text{SUC}_{i,t,s} \right) \right] \quad (1)$$

$$\text{Cost}_{es,t,s} = \left[\pi_{op}^{E} \left(P_{ch,t,s}^{E} + P_{dis,t,s}^{E} \right) \right] + \left[\pi_{net,t,s}^{E} \left(P_{ch,t,s}^{E} - P_{dis,t,s}^{E} \right) \right] \quad (2)$$

$$\text{OCT}_{i,t,s} = a_i P_{i,t,s}^{\ 2} + b_i P_{i,t,s} + c_i I_{i,t,s} \quad (3)$$

$$\text{SUC}_{i,t,s} = \text{SU}_i I_{i,t,s} \left(1 - I_{i,t-1,s} \right) \quad (4)$$

Equation (2) shows the operation cost of the ESS in charging and discharging modes. The third part corresponds to the operation cost of thermal generation units that are expanded in (3). The fourth part represents the start-up cost of thermal generation units that are expanded in (4).

The minimization problem in this study is subjected to the thermal unit and system constraints, wind power plant and ESS constraints, and responsive load economic model and downside risk constraints which are described below.

1.2 Constraints

Operation constraints of thermal generation units:

Generated power of thermal unit i is limited by its upper and lower values as shown in (5).

$$P_i^{min} I_{i,t,s} \le P_{i,t,s} \le P_i^{max} I_{i,t,s} \tag{5}$$

Any increase or decrease in the power generation of thermal unit i at consecutive periods is bounded by RU_i and RD_i as shown in (6) and (7).

$$P_{i,t,s} - P_{i,t-1,s} \le RU_i \tag{6}$$

$$P_{i,t-1,s} - P_{i,t,s} \le RD_i \tag{7}$$

Minimum up and downtime limits of thermal generation units are modelled by constraints (8) and (9), respectively.

$$\left(X_{i,t-1,s}^{on} - T_i^{on}\right)\left(I_{i,t-1,s} - I_{i,t,s}\right) \ge 0 \tag{8}$$

$$\left(X_{i,t-1,s}^{off} - T_i^{off}\right)\left(I_{i,t,s} - I_{i,t-1,s}\right) \ge 0 \tag{9}$$

1.3 Network reserve constraints:

The values of operation reserve, spinning reserve, and up/ down regulation reserve enhanced by thermal generation are specified as (10) and (11). The constraints (12)-(15) present the corresponding reserve conditions.

$$R_{i,t,s}^{O} + R_{i,t,s}^{S} + R_{i,t,s}^{RU} I_{i,t,s} Min\left\{RU_i, P_i^{max} - P_{i,t,s}\right\} \tag{10}$$

$$R_{i,t,s}^{RD} \le I_{i,t,s} Min\left\{RD_i, P_{i,t,s} - P_i^{min}\right\} \tag{11}$$

$$\sum_{i=1}^{N_i} R_{i,t,s}^{O} \ge R_{t,s}^{O} \tag{12}$$

$$\sum_{i=1}^{N_i} R_{i,t,s}^{S} \ge R_{t,s}^{S} \tag{13}$$

$$\sum_{i=1}^{N_i} R_{i,t,s}^{RU} \ge R_{t,s}^{RU} \tag{14}$$

$$\sum_{i=1}^{N_i} R_{i,t,s}^{RD} \ge R_{t,s}^{RD} \tag{15}$$

1.4 Operation constraints of the EESS:

EESs can be effective in operation costs. In the following, (16)-(21) models the operation of the electrical storage system.

$$\mathrm{P}_{\mathrm{storage,t,s}}^{\mathrm{E}} = \mathrm{P}_{\mathrm{storage,t-1,s}}^{\mathrm{E}} + P_{ch,t,s}^{E} \eta_{ch}^{E} - P_{dis,t,s}^{E} / \eta_{dis}^{E} - \mathrm{P}_{\mathrm{loss,t,s}}^{\mathrm{E}} \tag{16}$$

$$\mathrm{P}_{\mathrm{loss,t,s}}^{\mathrm{E}} = \vartheta_{loss}^{E} \mathrm{P}_{\mathrm{storage,t,s}}^{\mathrm{E}} \tag{17}$$

$$\alpha_{min}^{E} P_{CAPA}^{E} \le P_{storage,t,s}^{E} \le \alpha_{\max}^{E} P_{CAPA}^{E} \tag{18}$$

$$\beta^{E}_{min} P^{E}_{CAPA} \left(1/\eta^{E}_{ch}\right) I^{E}_{ch,t,s} \le P^{E}_{ch,t,s} \le \beta^{E}_{max} P^{E}_{CAPA} \left(1/\eta^{E}_{ch}\right) I^{E}_{ch,t,s} \quad (19)$$

$$\beta^{E}_{min} P^{E}_{CAPA} \eta^{E}_{dis} I^{E}_{dis,t,s} \le P^{E}_{dis,t,s} \le \beta^{E}_{max} P^{E}_{CAPA} \eta^{E}_{dis} I^{E}_{dis,t,s} \quad (20)$$

$$0 \le I^{E}_{dis,t,s} + I^{E}_{ch,t,s} \le 1 \quad (21)$$

Constraint (16) indicates that the electrical state of charge in each hour is a function of the prior state of charge, electrical charge, electrical discharge, and power loss in each hour and scenario. Furthermore, Constraint (17) shows that the power loss is equal to the percentage of the electrical state of charge. Constraint (18) shows that the electrical state of charge should be between the predefined minimum and maximum values. Moreover, the amounts of charge and discharge in each hour are limited to a predefined percentage of electrical energy storage capacity by (19) and (20). Constraint (21) indicates that the electrical energy storage unit can't simultaneously be on and off.

1.5 DC load flow constraints:

The power balance equation in each bus is given by (22). Power transmission from bus b to bus b' is determined in (23). The transmission line capacity limit is dictated by (24).

$$\sum_{i \in b} P_{i,t,s} + \sum_{r \in b} P_{r,t,s} + \sum_{h \in b} P^{E}_{ch,t,s} - \sum_{h \in b} P^{E}_{dis,t,s} - \sum_{b'=1}^{N_b} PF_{b,b',t,s} = Demand^{DR}_{b,t,s} \quad (22)$$

$$PF_{b,b',t,s} = \frac{(\delta_{b,t,s} - \delta_{b',t,s})}{X_{b,b'}} \quad (23)$$

$$\left| PF_{b,b',t,s} \right| \le PF^{max}_{b,b'} \quad (24)$$

1.6 Responsive load economic model

To formulate the participation of customers in DR programs, an economic load model that represents the changes in customer demand regarding the changes in electricity prices is expressed here.

$$D^{DR}_{b,t,s} = D^{base}_{b,t,s} \left\{ 1 + \sum_{\substack{j=1 \\ j \ne i}}^{24} E_{t,j} \left[\rho_j - \frac{\rho^0_j}{\rho^0_j} \right] \right\} \quad (25)$$

1.7 Dispatched wind power:

The probability distribution function (PDF) of the normal distribution is given as:

$$PDF(\varepsilon) = \frac{1}{\sigma\sqrt{2\pi}} exp\left(-\frac{(\varepsilon - \varepsilon_0)^2}{2\sigma^2} \right) \quad (26)$$

Each uncertainty parameter should be modelled with an appropriate PDF. The wind power generation forecast error can be represented by a normal distribution function. Moreover, the normal PDF has been used to model the demand. The limit of dispatched wind power is the only wind power plant constraint given by (27).

$$0 \le P_{r,t,s} \le P^{F}_{r,t,s} \quad (27)$$

2. DOWNSIDE RISK CONSTRAINTS (DRC)

As mentioned, risk management is essential for optimal operation. A robust and straightforward risk management method is required in power procurement problems.

Thus, in this section, the constraints that show the relationship between the risk and the expected operation cost are expressed. Electricity operators seek to reduce their power procurement cost to a lesser than a specified cost that is the operator's desired cost ($Target\_cost$).

The favourable scenarios for electricity operators are the scenarios in which the operator's power cost is less than the desired cost (Target _cost). Therefore, scenarios with higher operating costs can be defined as downside risks. Hence, to find the risk of non-desired (downside risk) scenarios, when the objective is the cost function, the DRC can be modelled as follows:

$$\begin{cases} Cost_s > Target\_\cos t & then \quad Risk_s = Cost_s - Target\_\cos t \\ Cost_s \le Target\_\cos t & then \quad Risk_s = 0 \end{cases} \tag{28}$$

In (28), $Cost_s$ and $Risk_s$ are power procurement cost and risk-in-cost of electricity operator in s^{th} scenario, respectively. Note that risk-in-cost is the subtraction between the costs of each scenario with the target cost. Constraint (28) can be rewritten mathematically linear as follows:

$$0 \le Risk_s - \left(Cost_s - Target\_\cos t\right) \le M_1\left(1 - U_s\right) \tag{29}$$

$$0 \le Risk_s \le M_2 U_s \tag{30}$$

In (29) and (30), M_1 and M_2 are high and positive constant amounts and U_s is a binary variable that is equal to 1 if$Cost_s >$ ($Target\_cost$). Otherwise, it is equal to 0.

By the mentioned context, the expected downside risk (EDR) for the power procurement cost function can be mathematically formulated as follows:

$$\sum_{s=1}^{S} w_s Risk_s \le \gamma EDR \tag{31}$$

$$EDR = \sum_{s=1}^{S} w_s \left(Cost_s^{No\ risk} - Target\_\cos t\right) \tag{32}$$

In (31), $Cost_s^{No\ risk}$ is the total cost in each scenario without considering the DRC. γ is the fixed coefficient that has an amount between 0 to 1, which is named the risk control coefficient. Finally, EDR is the expected downside risk. In the proposed method, by adding the proposed constraints to the primary formulation (1)-(27), the new problem is solved iteratively for different amounts ofγ; therefore, the obtained results report a different risk strategy with different risk and cost.

3. NUMERICAL STUDIES

In this section, first, the required data will be presented, and then analytical results are demonstrated.

3.1 Data

In this study, the proposed stochastic model, considering the responsive load economic model (RLEM), an EES system, and WG is evaluated on a six-bus system that is shown in Fig. 2. In the proposed system, the wind generation and electrical energy storage system (EESS) are located on bus 6. The 6-bus system consists of three thermal units, three electric loads, seven transmission lines, an EES system, and a wind power plant. The specifications of the thermal units, network load, transmission lines, and wind power generation are adopted from (Yu et al., 2019). The required minimum operating, spinning, and regulation reserves are set at 10, 5, and 2% of the network load, respectively.

In this paper, since wind energy and demand face uncertainties, the Bayesian probabilistic method is applied to produce the scenario tree. For each uncertain parameter,

scenarios are generated using the normal distribution. Considering the large number of generated scenarios, a clustering approach may be appropriate in such cases. Therefore, the K-Means clustering algorithm is used to reduce the number of total scenarios to 5 with a different probability. Selected scenarios by the K-Means clustering algorithm for demand and wind power are shown in Fig. 3 and Fig. 4, respectively.

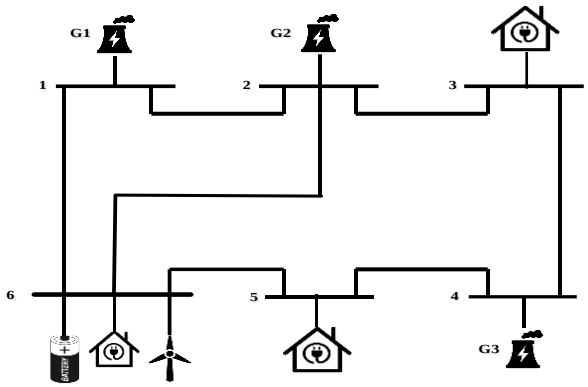

Figure 2. Illustration of 6-bus system.

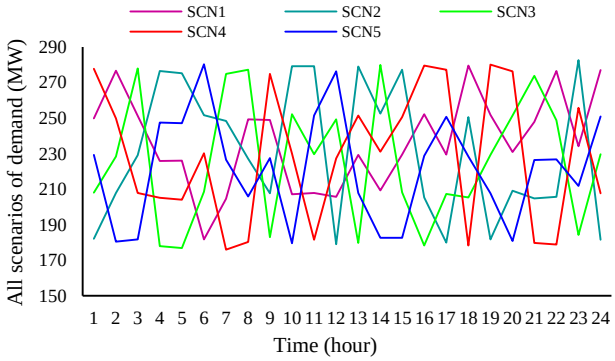

Figure 3.Selected demand scenarios

3.2 Analysis of results

In this study, a risk-constrained stochastic optimization approach is used to assess the impacts of uncertain variables on the system's risk. The downside risk constraint method (DRC) is applied to evaluate risk related to uncertainties. To reduce risk-in-cost, the risk-averse strategy is proposed instead of the risk-neutral strategy. To evaluate the effect of this approach on the proposed problem, two cases are presented as follows:

Case 1: Stochastic optimization problem of the desired system without downside risk constraints (risk-neutral strategy).

Case 2: Stochastic optimization problem of the desired system with downside risk constraints (risk-averse strategy).

Case 1 is a conventional stochastic programming problem in which the objective function is minimizing the expected operation cost. This case represents the risk-neutral strategy whose results can be seen in Table 1. In this table, the probability of each scenario, risk-in-cost, and operation cost of the system are represented, respectively. The average amounts of system operation cost and risk-in-cost in the risk-neutral strategy for 5 scenarios can be found in Table 1, which are $5530 and $5769, respectively. Risk-in-cost is defined as the difference between the operation cost in each scenario and the expected operating cost.

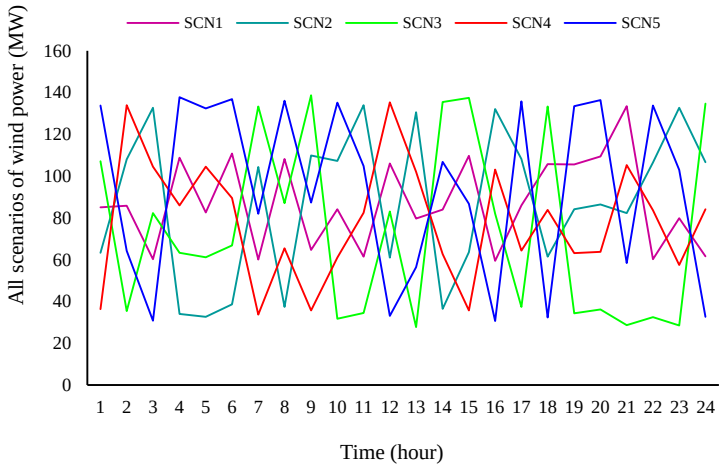

Figure 4. Selected wind power scenarios

Table.1. Results of the risk-neutral strategy without DRC (case1)

S	**Probability**	**Risk-in-cost ($)**	**Operation cost ($)**
SCN1	0.2	7037	4262
SCN2	0.16	1023	10276
SCN3	0.27	6966	4333
SCN4	0.18	5446	5853
SCN5	0.19	7037	4262
Expected	1	5769	5530

The risk-in-cost is reduced in Case 2 by implementing DRC as a risk-averse strategy. The positive results of this method are shown in Tables 2 and 3 (risk-averse strategies). Table 2 and Table 3 present, respectively, the operation cost and risk-in-cost in each scenario for the various amounts of the risk control parameter (γ). The key results are indicated in the last row of Table 2, at$\gamma = 0$. In this row, the cost of all scenarios reaches \$11300.000, thus $\gamma = 0$ is a scenario-independent strategy. Also, it can be concluded from Table 3 that the risk-in-cost in some scenarios is zero, as the operation cost is less than the expected operating cost. In Table 4, the expected risk-in-cost, the expected risk-in-cost reduction, the expected operation cost, and the expected operation cost increase for different amounts of the risk control parameter (γ) are presented. According to Table 4, the implementation of DRC for various amounts of the risk control parameter in Case 2 will result in a significant decrease in the risk-in-cost of the system, while the expected operation cost gradually increases. For example, by observing the data from $\gamma = 0.8$ to $\gamma = 0.7$ in Table 4, we can see that the risk-in-cost decreases by about 10%, while the expected cost increases by 0.1043%. Moreover, the Pareto optimal front between the expected operation cost and the expected risk-in-cost in Case 2 for different amounts of γ is depicted in Fig. 5.

Table. 2. The operation cost in each scenario versus the risk control parameter in case 2 ($)

s / γ	***SCN1***	***SCN2***	***SCN3***	***SCN4***	***SCN5***
1	4262.901	10276.276	4333.790	5853.894	4262.901
0.9	4312.315	9592.995	5589.906	6229.149	5682.318
0.8	5121.371	9814.432	5731.145	6483.082	7239.478
0.7	6777.378	9183.407	5726.694	6985.640	8594.467
0.6	7106.417	9090.906	7710.368	9650.247	6019.283
0.5	10925.617	8176.191	7100.366	10633.675	5741.082
0.4	7604.922	7202.324	10715.250	7852.813	10590.756
0.3	11300.000	11300.000	8773.940	8811.844	8137.223
0.2	10261.415	10422.009	9700.036	9477.232	11059.978
0.1	10703.252	11300.000	9605.205	11300.000	11300.000
0	11300.000	11300.000	11300.000	11300.000	11300.000

Table.3. the risk-in-cost in each scenario versus the risk control parameter in case 2 ($)

S / γ	**SCN1**	**SCN2**	**SCN3**	**SCN4**	**SCN5**
1	7037.099	1023.724	6966.210	5446.106	7037.099
0.9	6987.685	1707.005	5710.094	5070.851	5617.682
0.8	6178.629	1485.568	5568.855	4816.918	4060.522
0.7	4522.622	2116.593	5573.306	4314.360	2705.533
0.6	4193.583	2209.094	3589.632	1649.753	5280.717
0.5	374.383	3123.809	4199.634	666.325	5558.918
0.4	3695.078	4097.676	584.750	3447.187	709.244
0.3	0	0	2526.060	2488.156	3162.777
0.2	1038.585	877.991	1599.964	1822.768	240.022
0.1	596.748	0	1694.795	0	0
0	0	0	0	0	0

Table. 4. Analytical results versus risk control parameter

γ	**Expected risk-in-cost ($)**	**Total risk-in-cost ($)**	**%Expected risk-in-cost reduction**	**Expected operation cost ($)**	**Expected cost increase**
1	5769.440	27510.238	0	5530.560	0
0.9	5192.496	25093.317	10.00	6107.504	0.1043
0.8	4615.552	22110.492	20.00	6684.448	0.2086
0.7	4038.608	19232.414	30.00	7261.392	0.3129
0.6	3461.664	16922.779	40.00	7838.336	0.4172
0.5	2884.720	13923.069	50.00	8415.280	0.5215
0.4	2307.776	12533.935	60.00	8992.224	0.6259
0.3	1730.832	8176.993	70.00	9569.168	0.7302
0.2	1153.888	5579.33	80.00	10146.112	0.8345
0.1	576.944	2291.543	90.00	10723.056	0.938
0	0	0	100.00	11300.000	1.043

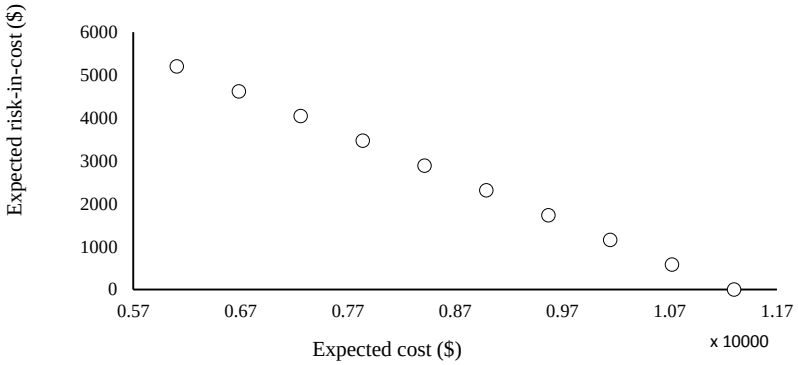

Figure 5. Pareto front among the expected cost and the expected risk-in-cost

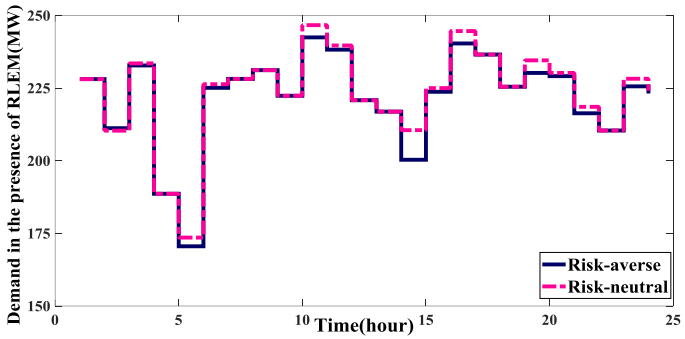

Figure 6. Risk-based network demand considering responsive load economic model (RLEM)

Fig. 6 shows changes in electricity demand under uncertain parameters for risk-averse and risk-neutral strategies. According to this figure, in the risk-averse strategy, in which the DRC is applied, electricity demand in some periods is lower than in the risk-neutral strategy, in which the DRC is not applied. Fig. 7 displays the risk-based scheduled power of three thermal generation units in risk-neutral and risk-averse strategies. Based on this figure, the scheduled power of the second unit is zero in both case studies. Fig. 8 illustrates the risk-based power of the electrical energy storage system.

This figure shows that compared to the risk-neutral strategy, in the risk-averse strategy, the power of the storage is only different in hours 7, 8.

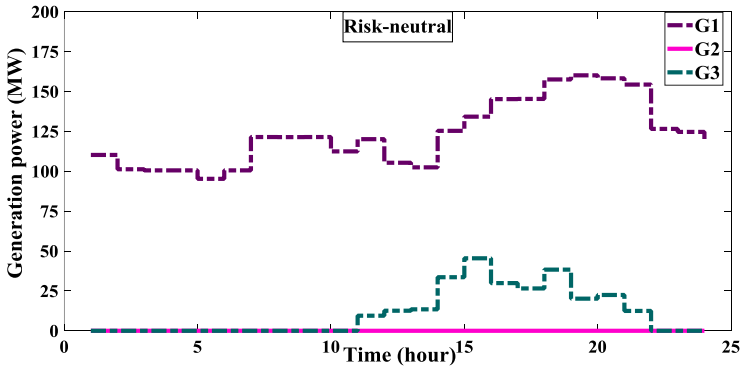

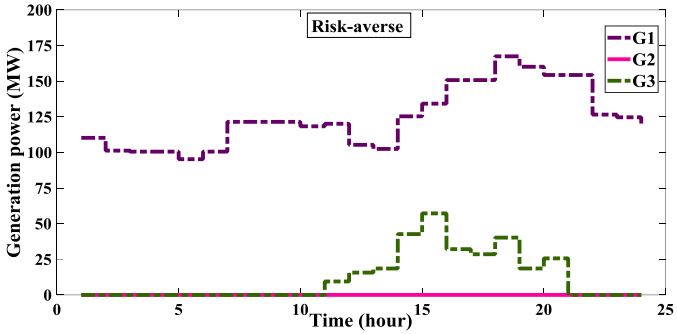

Figure 7. Risk-based scheduled power of thermal generation units

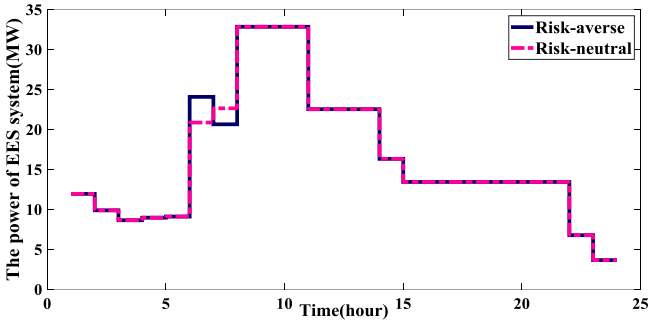

Figure 8. Risk-based power of the electrical energy storage system (EESS)

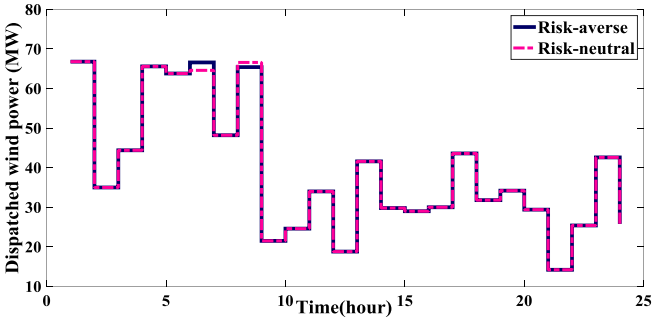

Figure 9.Risk-based scheduled power of wind generation

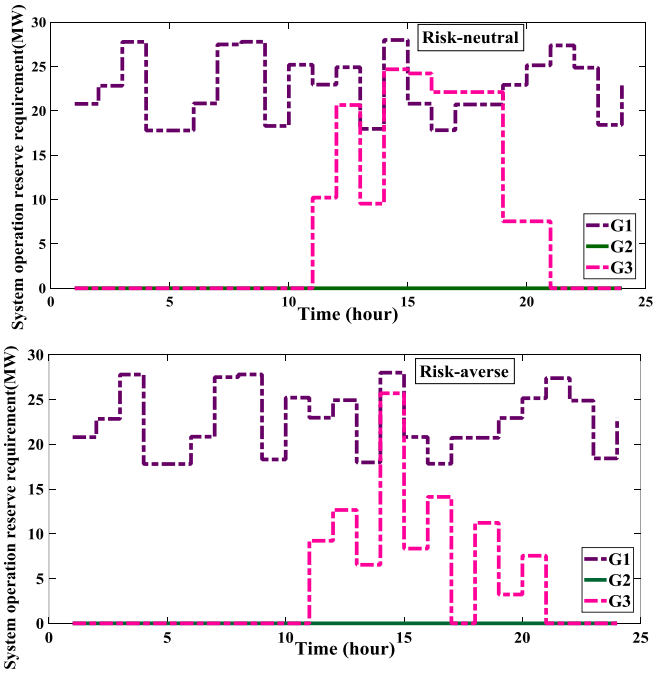

Figure 10. Risk-based system operation reserve requirement

Fig. 9 illustrates the risk-based dispatched power of wind generation in risk-neutral and risk-averse strategies. From that, we can determine that power values in the two strategies are different at hours 7 and 9. Furthermore, the system operation reserve requirements of three thermal generation units are indicated in both risk-neutral and risk-averse strategies in Fig. 10. In the risk-averse strategy, the operating reserve of the third thermal unit decreases at hours 13 and 14 as compared to the risk-neutral strategy.

CONCLUSIONS

In this paper, while considering the electrical energy storage system and responsive load economic model, a risk-constrained stochastic problem in the presence of various uncertainties was modelled. These uncertainties include wind power and electricity demand. Also, the downside risk-constraints method was used to control and evaluate the risks associated with these uncertainties. The results are presented for different amounts of the risk-control parameter, which indicates the expected cost and risk-in-cost amounts. By reducing γ from 1 to 0, the expected cost increased by 1.043%, while the risk-in-cost decreased by 100%. Therefore, it is concluded that while the anticipated operation cost of the system is gradually increasing, the risk-in-cost of the system will decrease significantly. Future research will focus on modelling the Power-to-Gas (P2G) systems.

REFERENCES

Aalami, H. A., Moghaddam, M. P., & Yousefi, G. R. (2010). Modeling and prioritizing demand response programs in power markets. *Electric Power Systems Research*, *80*(4), 426–435. https://doi.org/10.1016/j.epsr.2009.10.007

Beibei Wang, & Hobbs, B. F. (2013). Flexiramp market design for real-time operations: Can it approach the stochastic optimization ideal? *2013 IEEE Power & Energy Society General Meeting*, 1–5. https://doi.org/10.1109/PESMG.2013.6672220

Daneshi, H., & Srivastava, A. K. (2012). Security-constrained unit commitment with wind generation and compressed air energy storage. *IET Generation, Transmission & Distribution*, *6*(2), 167. https://doi.org/10.1049/iet-gtd.2010.0763

De Jonghe, C., Hobbs, B. F., & Belmans, R. (2014). Value of Price Responsive Load for Wind Integration in Unit Commitment. *IEEE Transactions on Power Systems*, *29*(2), 675–685. https://doi.org/10.1109/TPWRS.2013.2283516

Deng, T., Yan, W., Nojavan, S., & Jermsittiparsert, K. (2020). Risk evaluation and retail electricity pricing using downside risk constraints method. *Energy*, *192*, 116672. https://doi.org/10.1016/j.energy.2019.116672

Du, E., Zhang, N., Hodge, B.-M., Wang, Q., Kang, C., Kroposki, B., & Xia, Q. (2018). The Role of Concentrating Solar Power Toward High Renewable Energy Penetrated Power Systems. *IEEE Transactions on Power Systems*, *33*(6), 6630–6641. https://doi.org/10.1109/TPWRS.2018.2834461

Fotouhi Ghazvini, M. A., Faria, P., Ramos, S., Morais, H., & Vale, Z. (2015). Incentive-based demand response programs designed by asset-light retail electricity providers for the day-ahead market. *Energy*, *82*, 786–799. https://doi.org/10.1016/j.energy.2015.01.090

Hajibandeh, N., Shafie-khah, M., Talari, S., Dehghan, S., Amjady, N., Mariano, S. J. P. S., & Catalao, J. P. S. (2019). Demand Response-Based Operation Model in Electricity Markets With High Wind Power Penetration. *IEEE Transactions on Sustainable Energy*, *10*(2), 918–930. https://doi.org/10.1109/TSTE.2018.2854868

He, C., Zhang, X., Liu, T., Wu, L., & Shahidehpour, M. (2018). Coordination of Interdependent Electricity Grid and Natural Gas Network—a Review. *Current Sustainable/Renewable Energy Reports*, *5*(1), 23–36. https://doi.org/10.1007/s40518-018-0093-9

Heydarian-Forushani, E., Golshan, M. E. H., Shafie-khah, M., & Catalao, J. P. S. (2015). Impacts of stochastic demand response resource scheduling on large scale wind power integration. *2015 Australasian*

Universities Power Engineering Conference (AUPEC), 1–6. https://doi.org/10.1109/AUPEC.2015.7324857

Khodayar, M. E., Shahidehpour, M., & Wu, L. (2013). Enhancing the Dispatchability of Variable Wind Generation by Coordination With Pumped-Storage Hydro Units in Stochastic Power Systems. *IEEE Transactions on Power Systems*, *28*(3), 2808–2818. https://doi.org/10.1109/TPWRS.2013.2242099

Liu, G., & Tomsovic, K. (2014). A full demand response model in co-optimized energy and reserve market. *Electric Power Systems Research*, *111*, 62–70. https://doi.org/10.1016/j.epsr.2014.02.006

Marchenko, O. V., & Solomin, S. V. (2017). Modeling of hydrogen and electrical energy storages in wind/PV energy system on the Lake Baikal coast. *International Journal of Hydrogen Energy*, *42*(15), 9361–9370. https://doi.org/10.1016/j.ijhydene.2017.02.076

Navid, N., & Rosenwald, G. (2012). Market Solutions for Managing Ramp Flexibility With High Penetration of Renewable Resource. *IEEE Transactions on Sustainable Energy*, *3*(4), 784–790. https://doi.org/10.1109/TSTE.2012.2203615

Nazari-Heris, M., Abapour, S., & Mohammadi-Ivatloo, B. (2017). Optimal economic dispatch of FC-CHP based heat and power micro-grids. *Applied Thermal Engineering*, *114*, 756–769. https://doi.org/10.1016/j.applthermaleng.2016.12.016

Raj, N. T., Iniyan, S., & Goic, R. (2011). A review of renewable energy based cogeneration technologies. *Renewable and Sustainable Energy Reviews*, *15*(8), 3640–3648. https://doi.org/10.1016/j.rser.2011.06.003

Rong, A., & Lahdelma, R. (2016). Role of polygeneration in sustainable energy system development challenges and opportunities from optimization viewpoints. *Renewable and Sustainable Energy Reviews*, *53*, 363–372. https://doi.org/10.1016/j.rser.2015.08.060

Sahin, C., Shahidehpour, M., & Erkmen, I. (2013). Allocation of Hourly Reserve Versus Demand Response for Security-Constrained Scheduling of Stochastic Wind Energy. *IEEE Transactions on Sustainable Energy*, *4*(1), 219–228. https://doi.org/10.1109/TSTE.2012.2213849

Taljan, G., Fowler, M., Cañizares, C., & Verbič, G. (2008). Hydrogen storage for mixed wind–nuclear power plants in the context of a Hydrogen Economy. *International Journal of Hydrogen Energy*, *33*(17), 4463–4475. https://doi.org/10.1016/j.ijhydene.2008.06.040

Yu, D., Wang, J., Li, D., Jermsittiparsert, K., & Nojavan, S. (2019). Risk-averse stochastic operation of a power system integrated with hydrogen storage system and wind generation in the presence of demand response program. *International Journal of Hydrogen Energy*, *44*(59), 31204–31215. https://doi.org/10.1016/j.ijhydene.2019.09.222

A.SETS AND INDICES

t,j: The period's index

s: The scenarios index

b, b′: Index of buses

r: Index of wind power plant

i: Index of thermal units

es: Index of the EES system

N_t: Number of the period

N_s: Number of scenarios

N_b: Number of buses

N_r: Number of wind Generation

N_t: Number of the thermal generation unit

N_{es}: Number of the EES system

B.PARAMETERS

ω_s: The probability of scenarios

π_{op}^{E}: Electrical storage operation price

$\pi_{net,t,s}^{E}$: Electrical price at time t and scenario s

η_{ch}^{E}: The electrical storage charge efficiency

η_{dis}^{E}: The electrical storage discharge efficiency

ϑ_{loss}^{E}: The loss coefficient of electrical storage

α_{min}^{E}: The electrical storage minimum ratio

α_{max}^{E}: The electrical storage maximum ratio

β_{min}^{E}: The electrical storage minimum charge ratio

β_{max}^{E}: The electrical storage maximum charge ratio

a_i, b_i, c_i: Cost function coefficient of the thermal generation units

SU_i: The start-up cost of thermal unit i

P_i^{min}, P_i^{max}: Min/Max generation capacity of thermal unit i

$X_{b,b'}$: Reactance between bus b and b'

$PF_{b,b'}^{max}$: The maximum limit of exchanged power between bus b and b'

$D_{b,t,s}^{base}$: Initial demand value in t^{th} hour

$P_{r,t,s}^{F}$: Available wind power generation at time t and scenario s

$R_{t,s}^{O}, R_{t,s}^{S}$: Required operation and spinning reserves by the network

$R_{t,s}^{RU}, R_{t,s}^{RD}$: Required up and down-regulation reserves by the network

$\boldsymbol{E_{t,j}}$: cross elasticity

ρ_j: Spot electricity price in $\boldsymbol{t^{th}}$ hour (\$/kW h)

ρ_j^0: Initial electricity price in $\boldsymbol{t^{th}}$ hour (\$/ kW h)

$Target\_cost$: Predetermined cost

EDR: Expected downside risk

σ: The variance of the forecasted amount

γ: A number between 0 and 1 to control and assess risk

M_1, M_2: A positive and large amount

C.VARIABLES

$P_{ch,t,s}^{E}$: Electrical charge

$P_{dis,t,s}^{E}$: Electrical discharge

$\mathrm{P}_{\mathrm{storage,t,s}}^{\mathrm{E}}$: State of electrical energy storage

$P^{E}_{loss,t,s}$: Electrical loss

P^{E}_{CAPA}: The electrical storage capacity

RU_i, RD_i: Ramp up/down thermal unit i

T_i^{on}, T_i^{off}: Minimum up/downtime of unit i

$OCT_{i,t,s}$: The operation cost of the thermal generation unit

$SUC_{i,t,s}$: The start-up cost of the thermal generation unit

$P_{i,t,s}$: Produced power by the thermal generation unit

$X_{i,t,s}^{on}, X_{i,t,s}^{off}$: ON/OFF time of the thermal generation unit

$R_{i,t,s}^{O}, R_{i,t,s}^{S}$: Operation and spinning reserves provided by the thermal generation unit

$R_{i,t,s}^{RU}, R_{i,t,s}^{RD}$: Up and down-regulation reserves provided by the thermal generation unit

$P_{r,t,s}$: Dispatched wind power

$PF_{b,b',t,s}$: Exchanged power between bus b and b'

$Cost_{es,t,s}$: The total cost of electrical storage

$Cost_s^{No\ risk}$: Cost amount in each scenario without considering DRC

$Cost$: Expected operation cost

$\boldsymbol{Cost_s}$: Operation cost at the $\boldsymbol{s^{th}}$ scenario

$\boldsymbol{Risk_s}$: Risk cost at the $\boldsymbol{s^{th}}$ scenario

$\boldsymbol{D_{b,t,s}^{DR}}$: Demand in $\boldsymbol{t^{th}}$ hour

$\boldsymbol{\delta_{b,t,s}}$: Bus angle

$\boldsymbol{\varepsilon}$: Forecast error

D. BINARY VARIABLES

$I_{i,t,s}$: The binary variable that indicates the produced power by the thermal generation unit

U_s: Binary variable; it is equal to 1 when $Cost_s > Target\_cost$; otherwise, 0

$I_{ch,t,s}^{E}$: The binary variable of EESs charge

$I_{dis,t,s}^{E}$: The binary variable of EESs discharge